

NASA TECHNICAL NOTE



NASA TN D-8175

NASA TN D-8175

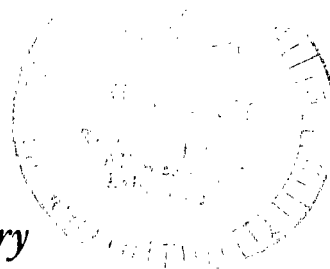


STREAKLINE FLOW VISUALIZATION
OF DISCRETE HOLE FILM COOLING
WITH HOLES INCLINED 30° TO SURFACE

LOAN COPY: RETURN TO
AFWL TECHNICAL LIBRARY
KIRTLAND AFB, N. M.

*Raymond S. Colladay, Louis M. Russell,
and Jan M. Lane*

*Lewis Research Center
and U.S. Army Air Mobility R&D Laboratory
Cleveland, Ohio 44135*





0133788

1. Report No. NASA TN D-8175		2. Government Accession No.		3. Recipient's Catalog No.	
4. Title and Subtitle STREAKLINE FLOW VISUALIZATION OF DISCRETE HOLE FILM COOLING WITH HOLES INCLINED 30° TO SURFACE				5. Report Date March 1976	
				6. Performing Organization Code	
7. Author(s) Raymond S. Colladay, Louis M. Russell, and Jan M. Lane				8. Performing Organization Report No. E-8570	
				10. Work Unit No. 505-04	
9. Performing Organization Name and Address NASA Lewis Research Center and U. S. Army Air Mobility R&D Laboratory Cleveland, Ohio 44135				11. Contract or Grant No.	
				13. Type of Report and Period Covered Technical Note	
12. Sponsoring Agency Name and Address National Aeronautics and Space Administration Washington, D. C. 20546				14. Sponsoring Agency Code	
15. Supplementary Notes					
16. Abstract Film injection from three rows of discrete holes angled 30° to the surface in line with the main-stream flow and spaced 5 diameters apart in a staggered array was visualized by using helium bubbles as tracer particles. Both the main stream and the film injectant were ambient air. Detailed streaklines showing the turbulent motion of the film mixing with the main stream were obtained by photographing small, neutrally buoyant helium-filled "soap" bubbles which followed the flow field. The ratio of boundary-layer thickness to hole diameter and the Reynolds number were typical of gas turbine film cooling applications. The results showed the behavior of the film and its interaction with the main stream for a range of blowing rates and two initial boundary-layer thicknesses.					
17. Key Words (Suggested by Author(s)) Flow visualization Film cooling Heat transfer Gas turbine			18. Distribution Statement Unclassified - unlimited STAR Category 34 (rev.)		
19. Security Classif. (of this report) Unclassified		20. Security Classif. (of this page) Unclassified		21. No. of Pages 16	
				22. Price* \$3.25	

STREAKLINE FLOW VISUALIZATION OF DISCRETE HOLE FILM COOLING WITH HOLES INCLINED 30° TO SURFACE

by Raymond S. Colladay, Louis M. Russell, and Jan M. Lane

Lewis Research Center and
U.S. Army Air Mobility R&D Laboratory

SUMMARY

Film injection from three rows of discrete holes angled 30° to the surface in line with the main-stream flow and spaced 5 diameters apart in a staggered array was visualized by using helium bubbles as tracer particles. Both the main stream and the film injectant were ambient air. Detailed streaklines showing the turbulent motion of the film mixing with the main stream were obtained by photographing small, neutrally buoyant helium-filled "soap" bubbles which followed the flow field. The ratio of boundary-layer thickness to hole diameter and the Reynolds number were typical of gas turbine film cooling applications. The results showed the behavior of the film and its interaction with the main stream for a range of blowing rates and two initial boundary-layer thicknesses.

INTRODUCTION

Air seeded with small neutrally buoyant helium-filled bubbles was injected into a turbulent boundary layer through discrete holes in the test surface of an ambient air wind tunnel. The path traced by the bubbles mapped streakline patterns of the injected film air mixing with the main stream. Test conditions simulated film cooling applications for gas turbines. To film cool turbine hardware operating in a high-heat-flux environment, it is important to inject film cooling air over the surface in the most efficient manner possible in order to provide the desired heat-transfer protection with a minimum disruption of the main stream. Poorly designed film injection schemes can lead to main stream momentum losses which severely reduce turbine aerodynamic efficiency and, in some instances, even increase heat transfer to the surface.

There has been considerable emphasis recently on experimental heat-transfer studies related to discrete hole film cooling. Erikson (ref. 1) and his predecessors at

the University of Minnesota investigated adiabatic wall film effectiveness and augmented heat-transfer coefficients due to blowing for one hole and a single row of holes at various injection angles and center-to-center spacings. Reference 1 is the last in a series of reports in this study. It includes a complete bibliography of earlier reports in the series. Liess (ref. 2) has made a similar study for a single row of injection holes with a free-stream static-pressure distribution typical of turbine blade applications. Crawford, Choe, Kays, and Moffat are investigating the heat-transfer characteristics of full coverage film cooling from a staggered array of discrete holes spaced either 5 or 10 diameters apart. Normal injection results from this study are presented in references 3 and 4, and reference 5 is a summary data report containing all the test results for both normal and 30° injection. Metzger, Takeuchi, and Kuenstler (ref. 6) examined surface averaged heat-transfer rates associated with a full coverage pattern of discrete holes oriented normal to the surface. Mayle and Camarata (ref. 7) investigated the adiabatic wall film effectiveness associated with full coverage film cooling from compound angle injection at various hole spacings. Analytical and experimental work in this same area has been the subject of several reports from Imperial College (refs. 8 and 9).

While all of these investigations have contributed to the quantitative data base needed to develop reliable analytical models of film cooling, they have also suggested the need for a better understanding of the complex fluid dynamics encountered when film air is injected through discrete holes into a turbulent boundary layer. Such insight can only be provided through good flow visualization studies. Some effort was made, as reported in reference 1, to visualize the flow field surrounding a single injection hole by using carbon dioxide fog. However, because of the high turbulent mixing in the injection region, the fog diffused so rapidly that only the large-scale turbulent motion near the hole was visible.

In the flow visualization technique described in this report detailed streaklines showing the turbulent motion of the injected secondary air are obtained by photographing very small neutrally buoyant helium-filled "soap" bubbles which follow the flow field. Unlike fog and smoke, which cannot preserve the details of the fluid motion because they diffuse rapidly, the bubbles form streaklines that are clearly identifiable as they pass downstream injection locations and can be traced back to their point of ejection.

Results are presented for one film injection hole geometry typical of turbine cooling applications, namely, three rows of holes angled 30° to the surface in the direction of the main stream in a staggered array with center-to-center spacing of 5 diameters. The momentum thickness Reynolds number at the first row of injection holes was 2165, and the ratio of boundary-layer thickness to hole diameter was 1.75. A ratio of boundary-layer thickness to hole diameter of 2.4 at the same Reynolds number was also obtained by moving the injection location farther downstream from the inlet nozzle.

SYMBOLS

D	film injection hole diameter
H	shape factor, δ^*/θ
m	ratio of film to main-stream velocity, or blowing rate
Re_θ	momentum thickness Reynolds number, $u_\infty \theta / \nu$
u	velocity
u_f	film injection velocity
u_∞	free-stream velocity
u^+	dimensionless velocity, $u/\sqrt{\tau_w/\rho}$
y	coordinate normal to surface
y^+	dimensionless distance, $y\sqrt{\tau_w/\rho}/\nu$
δ	boundary-layer thickness
δ^*	displacement thickness
θ	boundary-layer momentum thickness
ν	kinematic viscosity
ρ	density
τ_w	shear stress at wall

EXPERIMENTAL APPARATUS AND PROCEDURE

Bubble Generator

The bubble generator system, described in detail in the manufacturer's report (ref. 10), consists of a head that actually forms the bubbles and a console containing valves that control the flow of helium, bubble solution, and air to the head. A drawing illustrating the basic features of the head is shown in figure 1. Neutrally buoyant helium-filled bubbles, about 1 millimeter in diameter, form on the tip of the concentric tubes and are blown off the tip by a continuous blast of air flowing through the shroud passage. Bubble solution flows through the annular passage and is formed into bubbles inflated with the helium passing through the inner concentric tube. The desired bubble size and neutral buoyancy are achieved by proper adjustment of air, bubble solution, and helium flow rates. As many as 300 bubbles per second can be formed in this device.

Rig

The flow visualization test rig, consisting of a transparent plastic tunnel through which room air is drawn into a vacuum exhaust line, is a simple construction providing flexibility for testing a large number of hole injection geometries and boundary-layer configurations appropriate to turbine and combustor cooling applications. The test configuration for this report consisted of a zero-pressure-gradient main-stream flow over a flat surface containing discrete film injection holes. At the point of injection, the main-stream boundary layer was fully turbulent. A schematic showing the basic features of the test rig is shown in figure 2. There are three separate ambient airflow sources: (1) the primary main-stream air, (2) the bubble generator air, and (3) the secondary film injection air.

The tunnel, 0.381 by 0.152 meter in cross section, is sectioned into four parts: a test section 0.61 meter long and three spacing sections each 0.91 meter long. The sections may be placed in any order to allow for a boundary-layer development length upstream of the first film injection location anywhere from several centimeters to over 2.7 meters. Having the option of injecting the film air at different axial locations downstream of the inlet provides the flexibility of simultaneous control of the following parameters: ratio of injection to main-stream velocity u_f/u_∞ , ratio of injection hole diameter to boundary-layer thickness D/δ , and momentum thickness Reynolds number at the point of injection. A long boundary-layer development length is needed to cover the low range of D/δ because the minimum hole diameter is limited to about 1.27 centimeters to avoid excessive bubble breakage in the hole.

The neutrally buoyant helium-filled bubbles are injected into a plenum which serves as a collection chamber for the bubbles and the film air. The air, seeded with the bubbles, then passes through the film injection holes. The small quantity of air used by the bubble generator to blow the bubbles off the tip of the annulus as they form ends up as part of the film air in the plenum. However, this bubble airflow cannot be varied since it is adjusted and then fixed to give optimum bubble formation. Consequently, to provide variable film injection airflow rates, additional secondary air is also supplied to the plenum. The plenum box is clamped onto the bottom of the test section for easy removal when another test plate with a different hole configuration is to be tested. Rotameters were used to measure the helium and bubble generator airflow rates, and a hot wire flowmeter was used in the secondary air leg for accurate measurement over a wide range of film airflow rates.

The 0.38- by 0.61-meter floor of the test section which contains the film injection holes is easily removed to allow bottom plates with different hole configurations to be installed without affecting the rest of the test section or the plenum chamber. The test plate with the four holes angled 30° to the surface in line with the main stream is shown in figure 3. Tubes which extend into the plenum are inserted into the holes in the plate

and finished off flush with the test surface to provide a hole length-diameter ratio typical of aircraft turbine applications. The delivery tubes for this study were 1.27 centimeters in inside diameter and 6.35 centimeters long. The floor and back side of the test section are made of wood and have a glossy black finish to give maximum contrast with the bubble streaklines. A glossy black finish is preferred over a flat black finish to prevent diffuse reflection of the bubble streaks.

When the bubbles pass through the film injection holes, they are illuminated by a high-intensity quartz arc lamp. The resulting reflection off the bubble surface appears as a streak across the photographic film if the exposure is relatively long. The orientation of the light source is very important. Best results are achieved if the light beam can be directed axially down the tunnel as shown in figure 2. With a well focused and collimated light beam, the bubbles are illuminated as soon as they leave the holes without the beam striking any of the tunnel surfaces. This ensures good contrast with a bright bubble streak against a black background. The light source assembly is shown in figure 4. A high-efficiency, 300-watt quartz arc lamp gave sufficient light intensities for photographing the bubble streaks. A metal plate with a rectangular slot cutout was placed between the light source and the lens to mask the light beam, and an infrared reflecting filter was used to prevent heating of bubbles passing through the beam. The beam was then focused through a 300 millimeter lens to form a sharply defined rectangular light pattern having nominal dimensions of 7.7 by 15.2 centimeters at any axial location down the tunnel, wherever the test section was located.

RESULTS AND DISCUSSION

A fully turbulent boundary layer existed in the region of the film injection holes, and the free-stream turbulence intensity was 2 percent for all the results presented in this report. The ratio of film to main-stream velocity was varied by changing the mass flow rate of the secondary or film air while keeping the main-stream velocity constant at 15.5 meters per second. Results are presented for four ratios of film to main-stream velocity having nominal values of 0.3, 0.5, 0.8, and 1.4. The velocity profile through the boundary layer was surveyed just upstream of the injection holes. The dimensionless profile given in figure 5 shows the logarithmic distribution in the wall region, which is characteristic of a turbulent boundary layer on a smooth wall. The boundary-layer thickness defined by the 99-percent value of the free-stream velocity was 2.22 centimeters. Consequently, the ratio of boundary-layer thickness to injection hole diameter was 1.75 at the upstream injection location. The boundary-layer momentum thickness θ and shape factor H were 0.215 centimeter and 1.31, respectively, so the momentum thickness Reynolds number was 2165 at the upstream hole location.

Photographs of the film streaklines were taken both from the top looking down on the test surface and from the side looking through the boundary layer. The two viewing angles are illustrated in figure 6, which shows the test section with two cameras mounted in the positions used. The top views in figure 7 show the spreading characteristics of the film as it left the holes. The streaklines are black on a white background because the photographs are negative images printed from color transparencies. The side views in figures 8 to 10 show the degree of penetration of the film into the mainstream. Three different side views are included. Figure 8 is a full field view of the injection holes and the region extending downstream about 10 diameters. The boundary-layer thickness δ just upstream of the first injection hole is indicated on the left edge of each photograph. Figures 9 and 10 are closeup views of the regions surrounding the upstream and downstream holes, respectively. All the side photographs were taken with the two outer holes in the four hole array plugged and smoothed with modeling clay to give a plane view of the two center holes. The film from the upstream hole passed directly over the downstream hole.

A number of observations about the behavior of the film can be made from these figures:

(1) The top view shows that there was very little spreading of the film except at the highest blowing rate. At blowing rates of 0.3, 0.5, and 0.8, there was a slight tendency for the film to diverge when it encountered the film from the downstream injection hole directly in line with it. At the highest blowing rate, there was so much turbulent mixing that the downstream injection caused little additional perturbation of the upstream film.

(2) The counterrotating vortex pattern observed in normal injection (ref. 1) was not nearly as prominent for the slant hole injection. Evidence of this pattern can be seen in figure 7, however, which shows that as the streaklines came from the center of the hole they wrapped around the outside of the jet and entrained free-stream fluid down to the wall.

(3) At low blowing rates, as shown in figure 8(a) for $m = 0.3$, the film remained attached to the surface, and the streaklines were relatively smooth. There was an interwinding of streaklines on a scale much larger than the hole diameter.

(4) At the higher blowing rates (velocity ratios of 0.5 and greater) the film separated from the surface and allowed the main stream to wrap around and underneath the jets. The downstream jet penetrated farther into the main stream than the upstream jet, because the boundary layer had been thickened by the upstream injection.

(5) At all four blowing rates (figs. 8 to 10), the film jet briefly dipped back toward the wall at about 1 hole diameter downstream, but then proceeded on a trajectory which took it farther away from the surface.

(6) When the velocity ratio exceeded 1, the turbulent mixing became very high. Notice the kinks in the streaklines in part (d) of each of the figures. The tortuous paths

mapped out by the bubbles gives a measure of intensity of the turbulence generated by the injection process.

(7) At velocity ratios of 0.3, 0.5, and 0.8, figure 8 shows that the downstream film stayed underneath the incident film from the upstream hole, but the outer streaklines were not noticeably displaced.

(8) At the highest velocity ratio, 1.4, figures 8 and 10 show that the downstream film jet passed right up through the film from the upstream hole.

Another test configuration was run to determine the effect of the initial boundary-layer thickness on the distance that the film jet penetrates into the main stream. The test section was moved farther downstream from the inlet nozzle to provide a thicker boundary layer while at the same time the free-stream velocity was decreased to give the same Reynolds number at the point of injection. The boundary-layer thickness was increased 37 percent, and the blowing rate was 0.8, the same as for figure 8(c). A side view showing the streakline pattern is given in figure 11. The upstream film jet penetrated farther with the thicker boundary layer, but the penetration relative to the boundary-layer thickness was about the same (figs. 8(c) and 11). The trajectory of the downstream jet looked the same in both cases, which indicates that its penetration was controlled more by the upstream injection than the initial boundary-layer thickness.

CONCLUDING REMARKS

A film ejected from discrete holes at an angle to the surface but in line with the main stream remains discrete as the jets extend downstream. To provide good film coverage on the surface, holes should be spaced not more than 5 diameters apart, and much closer if only one or two rows of holes are used. If a large number of holes are used in a closely packed array, the design should be tailored with variable lateral and axial spacing to best utilize the cumulative buildup of film. An irregular staggered array may provide better film coverage than the regular staggered array tested in this study.

When the velocity ratio, or in general the mass velocity ratio, exceeds 0.5, the film separates from the surface and provides little or no protection from the main stream. Also, the high blowing rates generate excessive turbulent mixing, which dissipates the film, increases the heat flux, and increases aerodynamic losses in the turbine.

However, high injection velocities cannot be avoided in many turbine cooling designs because of the pressure drop needed across the wall to ensure that a positive flow direction is always maintained. Therefore, other hole geometries and angles must be studied

in order to provide a film that will remain attached to the surface in regions where high blowing rates are encountered.

Lewis Research Center,
National Aeronautics and Space Administration,
and
U. S. Army Air Mobility R&D Laboratory,
Cleveland, Ohio, December 17, 1975,
505-04.

REFERENCES

1. Erikson, V. L.: Film Cooling Effectiveness and Heat Transfer With Injection Through Holes. (HTL-TR-102, Minnesota Univ.; NAS3-13200.) NASA CR-72991, 1971.
2. Liess, Christian: Film Cooling With Ejection From a Row of Inclined Circular Holes. An Experimental Study for the Application to Gas Turbine Blades. VKI-TN-97, von Karman Inst. For Fluid Mechanics, 1973.
3. Choe, H.; Kays, W. M.; and Moffat, R. J.: The Superposition Approach to Film Cooling. ASME Paper 74-WA/HT-27, Nov. 1974.
4. Choe, H.; Kays, W. M.; and Moffat, R. J.: Turbulent Boundary Layer on a Full-Coverage Film-Cooled Surface - An Experimental Heat Transfer Study With Normal Injection. NASA CR-2642, 1975.
5. Crawford, M. E.; et al.: Full-Coverage Film Cooling Heat Transfer Study - Summary of Data for Normal-Hole Injection and 30° Slant-Hole Injection. NASA CR-2648, 1976.
6. Metzger, D. E.; Takeuchi, D. I.; and Kuenstler, P. A.: Effectiveness and Heat Transfer With Full-Coverage Film Cooling. J. Eng. Power, Trans. ASME, ser. A, vol. 95, no. 3, July 1973, pp. 180-184.
7. Mayle, R. E.; and Camarata, F. J.: Multihole Cooling Film Effectiveness and Heat Transfer. ASME Paper 74-HT-9, July 1974.
8. LeBrocq, P. V.; Launder, B. E.; and Priddin, C. H.: Experiments on Transpiration Cooling. I - Discrete Hole Injection as a Means of Transpiration Cooling: An Experimental Study. Inst. Mech. Engrs. Proc., vol. 187, no. 17, Apr. 1973, pp. 149-157.

9. Launder, B. E.; and York, J.: Discrete-Hole Cooling in the Presence of Free-stream Turbulence and a Strong Favorable Pressure Gradient. Int. J. Heat Mass Transfer, vol. 17, no. 11, Nov. 1974, pp. 1403-1409.
10. Hale, P. W.; et al.: Development of an Integrated System for Flow Visualization in Air Using Neutrally-Buoyant Bubbles. SAI-RR-7107, Sage Action, Inc., 1971.

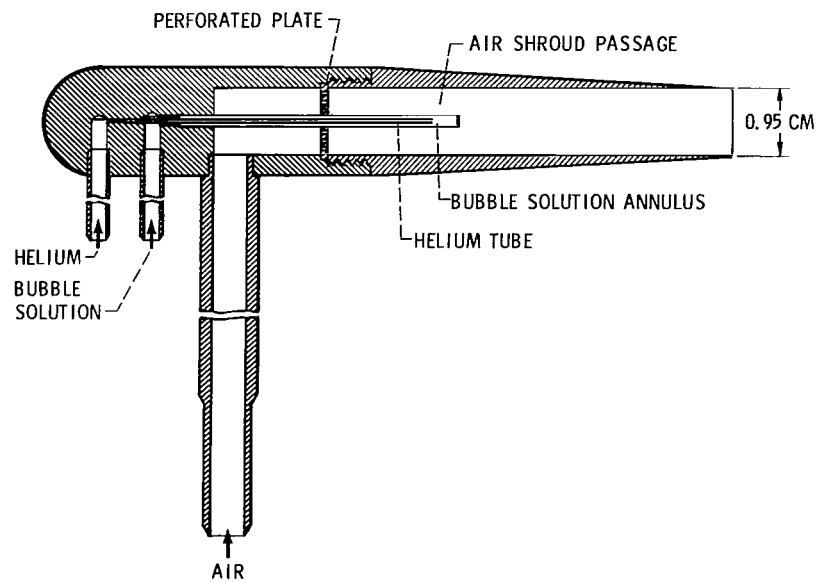


Figure 1. - Bubble generator head.

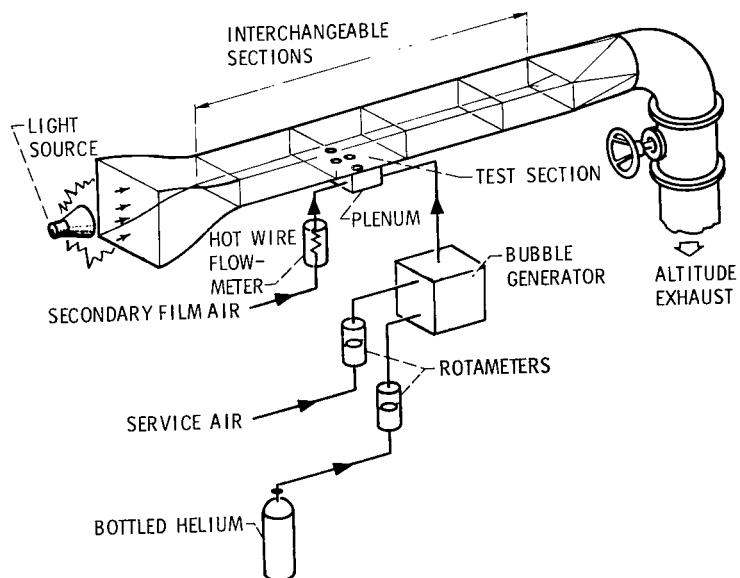


Figure 2. - Film cooling flow visualization rig.

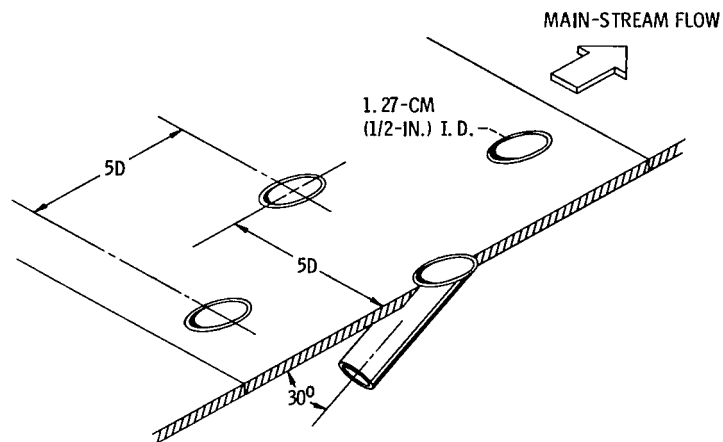


Figure 3. - Film injection test plate.

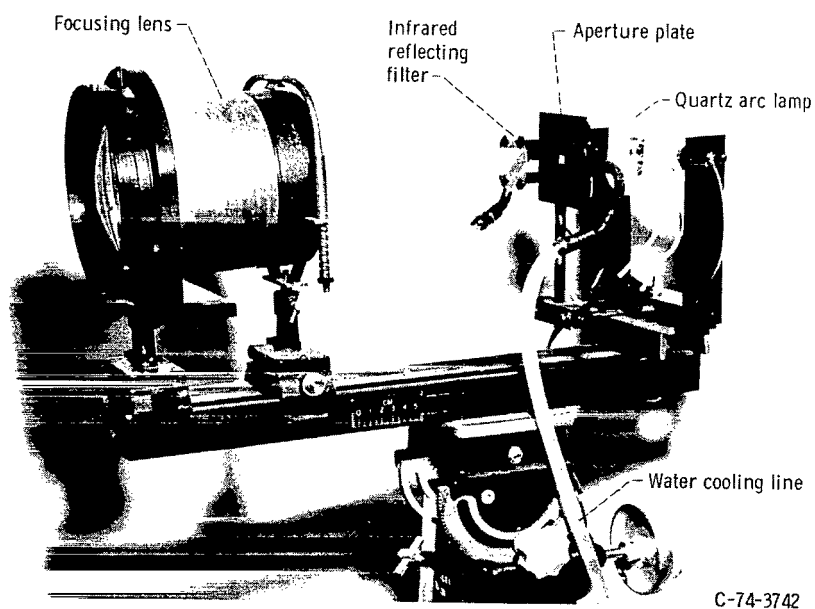


Figure 4. - Light source assembly.

C-74-3742

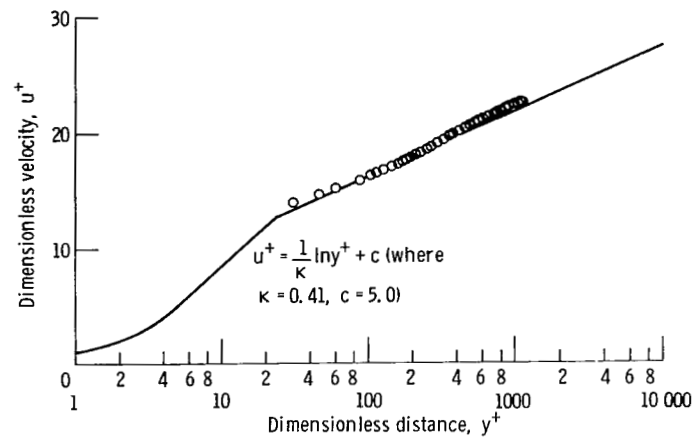


Figure 5. - Boundary-layer profile at upstream injection location.

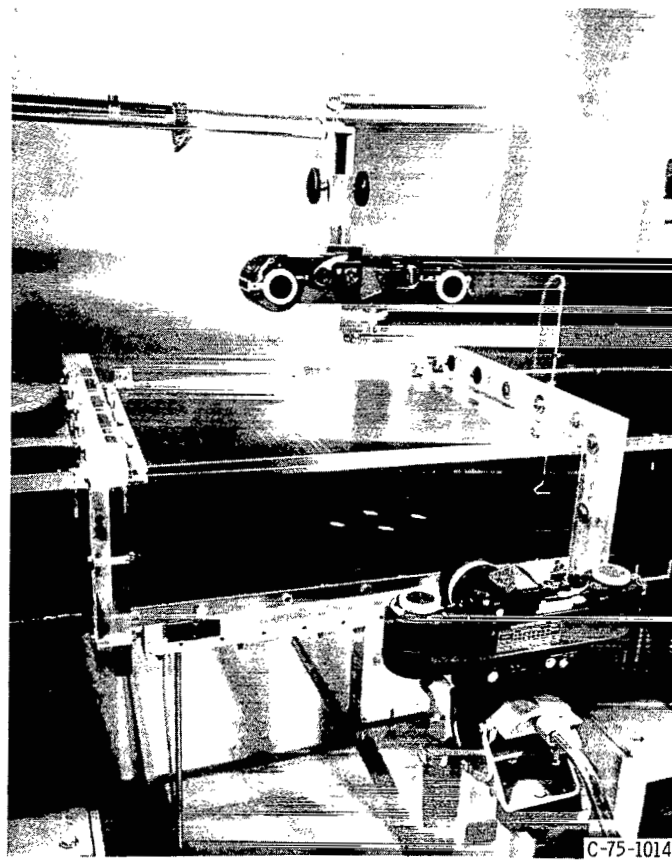
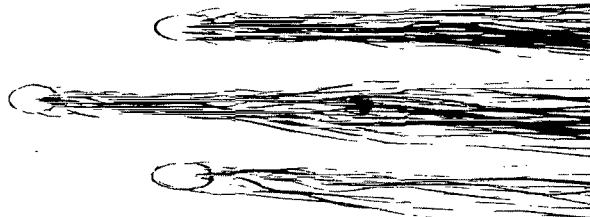


Figure 6. - Test section cameras in position for top and side views.



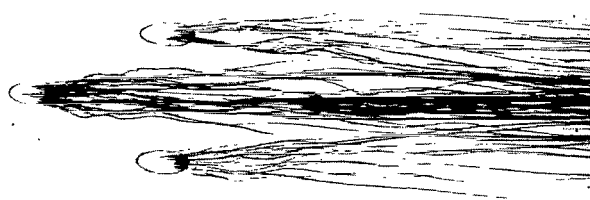
(a) Velocity ratio, 0.31.



(b) Velocity ratio, 0.50.



(c) Velocity ratio, 0.81.



(d) Velocity ratio, 1.40.

Figure 7. - Top views of streaklines.



(a) Velocity ratio, 0.30.



(b) Velocity ratio, 0.50.



(c) Velocity ratio, 0.80.



(d) Velocity ratio, 1.40.

Figure 8. - Full field side views of streaklines.



(a) Velocity ratio, 0.30.



(b) Velocity ratio, 0.50.



(c) Velocity ratio, 0.86.



(d) Velocity ratio, 1.42.

Figure 9. - Closeup side views of streaklines from upstream hole.



(a) Velocity ratio, 0.30.



(b) Velocity ratio, 0.48.



(c) Velocity ratio, 0.80.



(d) Velocity ratio, 1.40.

Figure 10. - Closeup side views of streaklines from downstream hole.



Figure 11. - Streaklines during injection into thick boundary layer at velocity ratio of 0.80.



334 001 C1 U D 760220 S00903DS
DEPT OF THE AIR FORCE
AF WEAPONS LABORATORY
ATTN: TECHNICAL LIBRARY (SUL)
KIRTLAND AFB NM 87117

Deliverable (Section 158
Postal Manual) Do Not Return

"The aeronautical and space activities of the United States shall be conducted so as to contribute . . . to the expansion of human knowledge of phenomena in the atmosphere and space. The Administration shall provide for the widest practicable and appropriate dissemination of information concerning its activities and the results thereof."

—NATIONAL AERONAUTICS AND SPACE ACT OF 1958

NASA SCIENTIFIC AND TECHNICAL PUBLICATIONS

TECHNICAL REPORTS: Scientific and technical information considered important, complete, and a lasting contribution to existing knowledge.

TECHNICAL NOTES: Information less broad in scope but nevertheless of importance as a contribution to existing knowledge.

TECHNICAL MEMORANDUMS: Information receiving limited distribution because of preliminary data, security classification, or other reasons. Also includes conference proceedings with either limited or unlimited distribution.

CONTRACTOR REPORTS: Scientific and technical information generated under a NASA contract or grant and considered an important contribution to existing knowledge.

TECHNICAL TRANSLATIONS: Information published in a foreign language considered to merit NASA distribution in English.

SPECIAL PUBLICATIONS: Information derived from or of value to NASA activities. Publications include final reports of major projects, monographs, data compilations, handbooks, sourcebooks, and special bibliographies.

TECHNOLOGY UTILIZATION PUBLICATIONS: Information on technology used by NASA that may be of particular interest in commercial and other non-aerospace applications. Publications include Tech Briefs, Technology Utilization Reports and Technology Surveys.

Details on the availability of these publications may be obtained from:

SCIENTIFIC AND TECHNICAL INFORMATION OFFICE

NATIONAL AERONAUTICS AND SPACE ADMINISTRATION

Washington, D.C. 20546